

Space-charge layer, metallization, and collective excitations of the Bi/GaAs(110) interface

Valentina De Renzi, Roberto Biagi, Maria Grazia Betti, and Carlo Mariani
Dipartimento di Fisica, Università di Modena, via G. Campi 213/A, I-41100 Modena, Italy
 (Received 6 August 1993; revised manuscript received 15 November 1993)

The collective excitations and the metallization of the Bi/GaAs(110) interface grown at room temperature, up to the completion of a few tens of a monolayer, have been studied by means of the high-resolution electron-energy-loss spectroscopy (HREELS). Through analysis of the HREELS data, also by means of an appropriate semiclassical dielectric model, the modifications experienced by the substrate-related loss structures (Fuchs-Kliwer phonon and dopant-induced free-carrier plasmon) and by the quasielastic peak are related to changes in the dielectric response of the overlayer and in the semiconductor space-charge region. The influence of bismuth is effective in enlarging the depletion layer thickness, leaving the interface semiconducting at the monolayer-coverage scale. A band bending value of 0.56 eV is obtained at the coverage of one monolayer on the highly n -type doped sample ($n \sim 2.7 \times 10^{18} \text{ cm}^{-3}$); a determination free from any possible surface photovoltaic effect. At coverages greater than two monolayers, which corresponds to a structural transition, the intermediate structural phase becomes metallic, thus marking a clear semiconductor-metal transition. This intermediate metallic stage further develops towards the formation of actual semimetallic crystalline bismuth layers oriented with the basal plane parallel to the substrate surface.

I. INTRODUCTION

Group-V semimetals deposited at room temperature (RT) on the (110) surface of III-V compound semiconductors constitute valuable examples of unreactive, nondisruptive, and ordered interfaces. These physical systems have been studied in great detail at the very first growth stage, around a coverage of one monolayer (ML), while a complete and exhaustive investigation of the interface evolution at higher thicknesses has not yet been achieved. Within this class of interfaces, Sb/GaAs(110) has been widely studied as a model system:¹⁻⁵ the interface evolution at RT is characterized by the formation of a uniform and epitaxial monolayer,¹ followed by island formation (Stransky-Krastanov growth mode) with amorphous character (up to about 15 ML),²⁻⁵ and eventually by the nucleation of bulklike crystallites of antimony.⁶ In correspondence to these structural phases, a clear modification of the dielectric properties from semiconducting to semimetallic has been identified on overcoming the coverage of 15 ML.^{2,5}

The Bi/GaAs(110) system is of interest also. It grows with three different structural phases up to the completion of a bulklike Bi film. However, in contrast to the Sb/GaAs(110) interface, it presents a *long-range* crystalline order in the whole thickness range (from the epitaxial monolayer to the bulklike bismuth crystal).^{7,8} The three growth phases are characterized by different crystalline order, morphology, and dielectric properties. Our purpose is to determine the dielectric properties of the system at the different structural stages of the interface, up to the bulklike phase. A great deal of information about the Bi/GaAs(110) system is already available, in particular for what concerns the first growth stage, i.e., at a Bi coverage lower than two monolayers (ML). Main works on this system were performed using photoemission^{9,10}

and inverse photoemission spectroscopy,^{11,12} scanning tunneling microscopy and spectroscopy (STM),^{7,10} low-energy electron diffraction (LEED),⁸ and high-resolution electron-energy-loss spectroscopy (HREELS).¹³ It is worthwhile to recall briefly the principal characteristics of the different growth phases, as achieved by the experimental techniques mentioned above: for submonolayer coverages Bi grows epitaxially on the GaAs(110) surface,⁸ forming zigzag chains along the $[1\bar{1}0]$ direction, in analogy to what has been observed for the Sb/GaAs(110) system.¹ However, these chains extend no longer than $\sim 24 \text{ \AA}$ in the $[1\bar{1}0]$ direction, as if to relieve the strain due to the Bi-substrate mismatch. On increasing coverage, these parallel chains coalesce into islands until a uniform epitaxial monolayer is formed.^{7,10} From the dielectric point of view, the 1-ML Bi/GaAs(110) system is still semiconducting, as the energy gap narrows from that of clean GaAs (1.4 eV) to 0.65 eV. This result has been accomplished by photoemission^{9,10} and inverse photoemission spectroscopies,^{11,12} STM,¹⁰ and HREELS (Ref. 13) measurements. Recent STM (Ref. 7) studies have shown that after the completion of the first Bi monolayer an island growth follows, with the formation of clusters on the epitaxial layer, presenting an average height of $\approx 7 \text{ \AA}$. These two dimensional (2D) islands crystallize in a surface lattice corresponding to a pseudocubic (110) plane, with thickness equivalent to the stacking of three such layers, and without exceeding a diameter of 300 \AA . Beyond 2 ML these 2D islands coalesce at RT, forming large three-dimensional (3D) crystallites, sweeping great areas of the (1×1) epilayer formerly free from 2D islands (Stransky-Krastanov growth). The 3D crystallites result to be very anisotropic in shape, as they are elongated along the $[1\bar{1}0]$ substrate direction. Although both structures (2D and 3D clusters) expose pseudocubic (110) surfaces, the 2D islands are three layers high, while the

height of the elongated crystallites is a multiple of two layers.⁷ As to the dielectric nature of the interface beyond 2 ML, the semiconductor gap closes and the system becomes semimetallic.^{8–12} Hence the thickness range 2–30 ML can be considered as a peculiar growth phase, intermediate between and different from both the epitaxial (~ 1 ML) and the fully 3D (≥ 30 ML) bulklike stage. It is intermediate insofar as its crystalline structure appears different from that of the other phases, and a semiconducting-semimetallic transition takes place in this coverage range. The peculiarity of this coverage stage is also outlined by its particular lattice dynamics singled out by Raman effect measurements.¹⁴ In any event, the proper dielectric and structural properties of this intermediate phase are still not fully determined. In the third growth stage (> 30 ML) a bulklike and almost single-crystalline growth of Bi is achieved, as shown by the hexagonal-like LEED pattern,⁸ and by the low-energy electronic properties studied by the HREELS technique.¹⁵ Moreover, interesting effects due to size quantization have been singled out up to a coverage of the order of 500 Å.¹⁶

In the general framework of the Bi/GaAs(110) system evolution on growing the bismuth thickness, outlined by these different experimental techniques, the present investigation carried out by HREELS was performed to study the dielectric properties of the interface and the subsurface space-charge region, at the different growth phases. In fact, thanks to the high surface sensitivity of HREELS, and to the high scattering efficiency of the vibrational and collective modes in the far-infrared energy range, it is possible to carefully investigate the evolution of the subsurface space-charge region of the substrate,¹⁷ up to the completion of the first growth phase (~ 1 ML Bi). In particular, this can be accomplished through the experimental study of the coupled Fuchs-Kliwer optical phonon and dopant-induced free-carrier plasmon, as a function of the Bi thickness. Moreover, by performing a model calculation using a semiclassical approach,¹⁸ it is possible to simulate the interface system as a sequence of uniform layers (each characterized by its proper modes), and to construct model spectra to fit the experimental data. As a consequence, the Bi-induced depletion layer and consequent band bending can be deduced in the low-coverage region, and the dielectric character of the system can be obtained, following the metallization process up to a coverage of a few tens of a monolayer.

The paper is organized as follows: after an experimental section (II), the data will be shown in Sec. III, while their analysis and discussion will be presented in the Sec. IV. The conclusions will be drawn in Sec. V.

II. EXPERIMENT

Experiments were carried out at the surface physics laboratory Spettroscopia Elettronica Superfici e Adsorbati (SESAMO) at the Dipartimento di Fisica, Università di Modena. The HREELS spectrometer (Leybold-Heraeus ELS-22) is contained in an ultrahigh-vacuum (UHV) chamber, also equipped with low-energy electron diffraction (LEED), x-ray photoemission spectroscopy

(XPS), and other spectroscopic tools. This system is UHV connected to a preparation chamber containing all ancillary facilities for sample preparation and characterization. Base pressure in both chambers was in the 10^{-11} -mbar (10^{-9} Pa) range, ensuring excellent conditions for the clean crystal growth and investigation. The Bi/GaAs(110) interface was obtained by evaporation of the semimetal from a resistively heated quartz crucible, with evaporation rate of the order of a few Å/min on freshly UHV-cleaved GaAs(110) surfaces, at room temperature (RT). Pressure rose in the low 10^{-10} mbar (10^{-8} Pa) during the evaporation. The overlayer thickness was determined with an oscillating quartz microbalance calibrated through XPS measurements. We have performed x-ray photoemission with an Al $K\alpha$ photon source in the binding-energy range 50–10 eV, for different stages of deposition. The coverage dependence of the Ga 3*d*, As 3*d*, and Bi 5*d* core-level intensities was analyzed and is reported in Fig. 1. The overlayer thickness calibration has been achieved comparing the *ratio* between the Ga and As peak intensities to that of Bi at each coverage step, with those of the 1 ML Bi/GaAs(110) system obtained after annealing a thin Bi film at 300°C for about 10 min. In fact, it is well known that heating a thick Bi layer for a few minutes at 300°C causes the desorption of Bi until only 1 ML remains stuck at the surface.¹⁹ The equivalent uniform thickness at 1 ML—as given by the oscillating quartz-crystal thickness monitor—was about 3 Å, corresponding to a Bi surface-atomic density equal to that of the GaAs(110) substrate ($\sim 8.85 \times 10^{14}$ at. cm^{-2}). The attenuation rate for Ga and As is slightly different, owing to the different kinetic energy and consequent mean free path of the outgoing photoelectrons. Moreover, the attenuation rate shows a linear behavior—indicative of epitaxial growth—until 1 ML is reached, while beyond this coverage a slowdown is clearly observed, marking a Stransky-Krastanov growth mode, as reported in previous photoemission works.^{9,10} The cleanness of the surface was checked by photoemission and by the HREELS spectra themselves; however, the system under investigation has been shown to be very unreactive in UHV conditions. HREELS measurements were taken in the specular direction, with primary beam energies (E_p) ranging from 5 to 20 eV, and with incident and collecting angles of about 65°. The energy resolution, defined as the full width at half maximum (FWHM) of the elastically scattered peak, was better than 10 meV, ensuring a precision of the order of 2 meV in the energy-shift measurements. Spectra were taken on two differently *n*-type (Te) doped GaAs samples, with a nominal concentration of 2.7×10^{18} cm^{-3} and 3×10^{16} cm^{-3} , respectively.

III. RESULTS

The intensity of the elastically scattered electrons out of a surface (i.e., the quasielastic peak in the HREELS spectra) is related to the surface reflectivity of the sample.¹⁷ It is therefore ruled by two principal factors: surface order and smoothness, and the surface dielectric response. Even if a quantitative and absolute evaluation

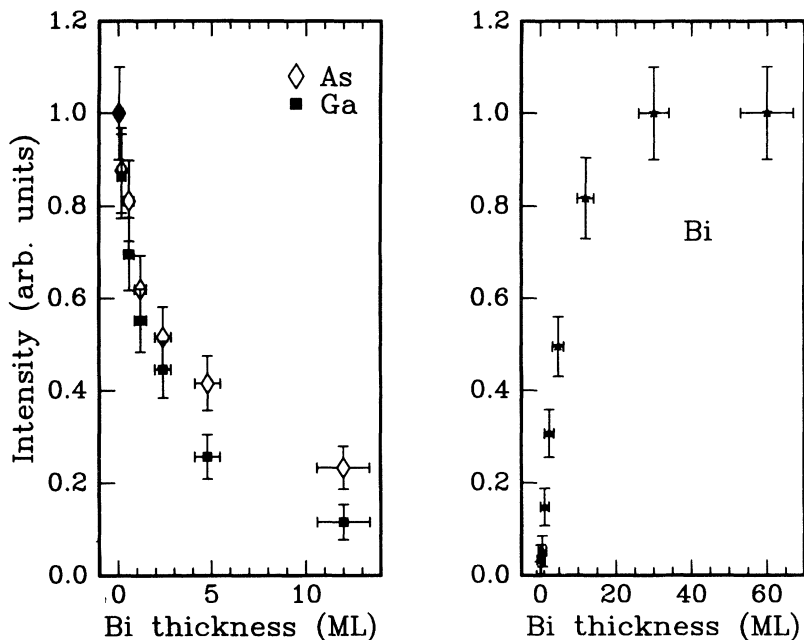


FIG. 1. XPS intensity of the As 3d, Ga 3d (left side), and Bi 5d (right side) core levels as a function of the Bi coverage.

of these factors is quite a difficult item, qualitative but valuable information on the dielectric nature and on the order of the Bi/GaAs(110) interface can be obtained by the analysis of the behavior of the quasielastic peak intensity as a function of coverage. This behavior was well reproducible in all series of measurements we have performed, and resulted in being quite peculiar, as can be observed in Fig. 2, where the elastic peak intensity vs Bi coverage is reported. The quasielastic peak intensity presents a pronounced dip for ~ 0.5 ML; thereafter it increases rather steeply, reaching a maximum at ~ 5 ML, where it becomes one order of magnitude greater than that of the clean surface (I_0). Above this coverage the intensity slowly decreases toward a constant lower value.

To obtain more quantitative information about the dielectric nature of the interface, we analyzed the coverage dependence of the energy-loss spectra also in the energy region of the phonon and the plasmon loss structures. The HREELS data for the higher doped sample

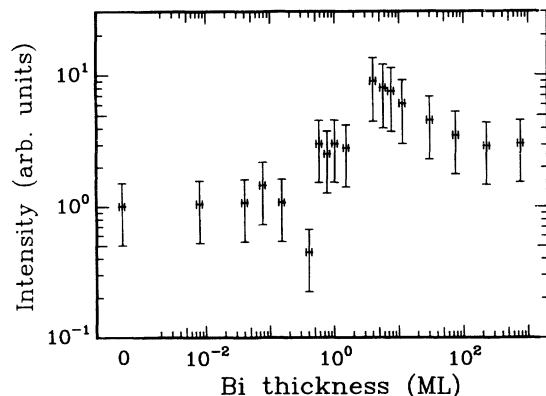


FIG. 2. Intensity of the quasielastic peak as a function of the Bi coverage.

taken at a primary beam energy of 20 eV are presented in Fig. 3 as a function of coverage (0–30 ML). The spectra show two intense features. The strongest is the plasmon-like excitation, and lies at about 62 meV for the clean surface: it is due to the oscillations of the n -type dopant-induced free carriers. The other structure is the Fuchs-Kliwer optical phonon of GaAs, lying at about 36 meV for the clean surface.²⁰ We have fitted the quasielastic

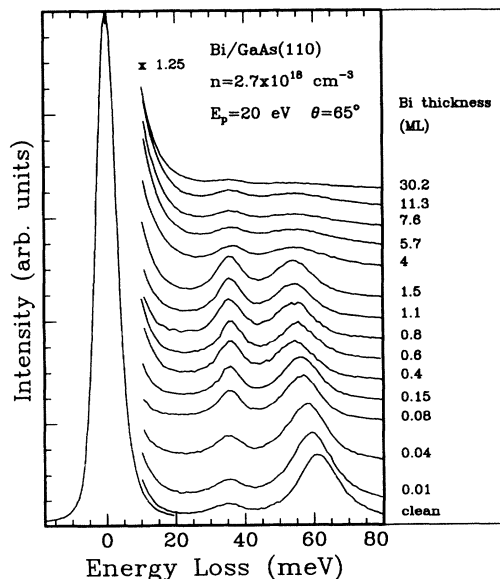


FIG. 3. High-resolution electron-energy-loss spectra of the Bi/[n -type GaAs(110)] interface system, as a function of the Bi coverage, in the energy region of the Fuchs-Kliwer optical phonon and of the dopant-induced free-carrier plasmon. Highly doped substrate, doping concentration $n = 2.7 \times 10^{18} \text{ cm}^{-3}$. Primary beam energy of 20 eV and angle of incidence of 65° . Spectra are normalized to their respective quasielastic peak heights, and displaced along the vertical axis for the sake of clarity.

peak and the phonon and plasmon structures through Lorentzian curves convoluted with a Gaussian, the latter to take into account the experimental broadening. From the results of this fitting procedure, we report in Fig. 4 the phonon and plasmon intensities thus evaluated, along with the plasmon energy, as a function of coverage. While the plasmon intensity begins to decrease at submonolayer coverages, the phonon peak increases as Bi grows up to 1 ML. After the completion of the first layer, both structures lose intensity and finally become almost indistinguishable from the background at about 30 ML. Moreover, while the phonon peak energy does not change with coverage, the plasmon peak undergoes a shift toward lower energies by about 7 meV (as Bi reaches 1 ML), then shifts back by 2 meV between 1 and 10 ML. In order to achieve more information about the dielectric evolution of the overlayer toward a semimetallic character, we have also performed HREELS measurements with a primary beam energy of 5 eV, on the lower doped sample. In these data the plasmon feature is centered at about 7 meV, resulting in being convoluted with the quasielastic peak, which consequently presents a 16-meV energy width. Beyond the decreasing intensity of the phonon peak upon Bi coverage, the most impressive feature for this series of measurements is the strong elastic peak-width dependence on coverage. We recall that, on covering a semiconducting substrate with a metallic overlayer, a coupling between the overlayer plasmon with the substrate phonon takes place, giving rise to two distinct excitations.²¹ In the limit of vanishing exchanged momentum q_{\parallel} (in the typical kinematic scattering conditions of a

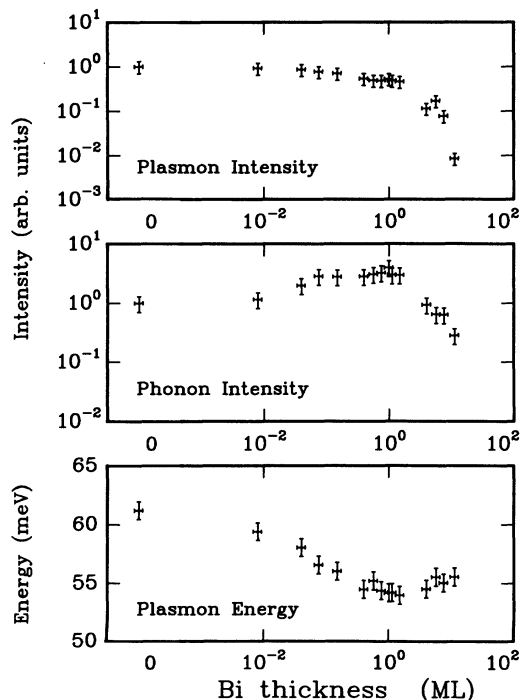


FIG. 4. From the top to the bottom: plasmon intensity, phonon intensity, and plasmon energy position, as a function of the Bi coverage. Data refer to the HREELS experiment performed on the highly doped substrate (and shown in Fig. 3).

HREELS experiment), the higher-energy mode is close to the phonon energy, while the lower-energy excitation is an acoustic mode with very low energy, which causes an elastic peak enlargement, followed by a narrowing, when the interface becomes fully metallic.²¹ In particular, this phenomenon is more evident when the acoustic mode presents a higher frequency, the latter proportional to the exchanged momentum, thus inversely proportional to the square root of the primary beam energy. Hence one can expect that, upon metallization, the absolute value of the elastic peak widening is inversely proportional to the primary beam energy (E_p). This is what we have observed and shown in Fig. 5, where the elastic peak width [evaluated as the full width at half maximum (FWHM) of the quasielastic peak] is reported as a function of the Bi coverage and of E_p . The Δ FWHM rises to 15 (for $E_p = 5$ eV) and 5 meV (for $E_p = 15.9$ eV), while it is almost zero for $E_p = 20$ eV, as expected.

The principal characteristics of the evolution of the HREELS data relative to the Bi/GaAs(110) interface on growing the overlayer thickness can be synthesized as follows. (i) The elastic peak intensity presents a peculiar behavior as a function of coverage, inasmuch as a drastic lowering (at ~ 0.5 -ML Bi) is followed by a remarkable increase (at ~ 5 -ML Bi). (ii) The attenuation of the phonon and plasmon structures is definite above ≈ 1 -ML coverage, along with the plasmon energy shift (by ≈ 7 meV) toward lower energy (at 1-ML Bi), reflecting the space-charge layer conditions. (iii) The elastic peak width shows a widening followed by a narrowing as a function of the Bi coverage, and its absolute value depends on the primary beam energy.

IV. ANALYSIS AND DISCUSSION

We have noticed that the elastic peak intensity I_0 depends on the order and on the dielectric nature of the scattering surface: since the system has been shown to remain semiconducting until 1 ML is completed,¹³ the dip observed for I_0 at 0.5 ML coverage (Fig. 2) can there-

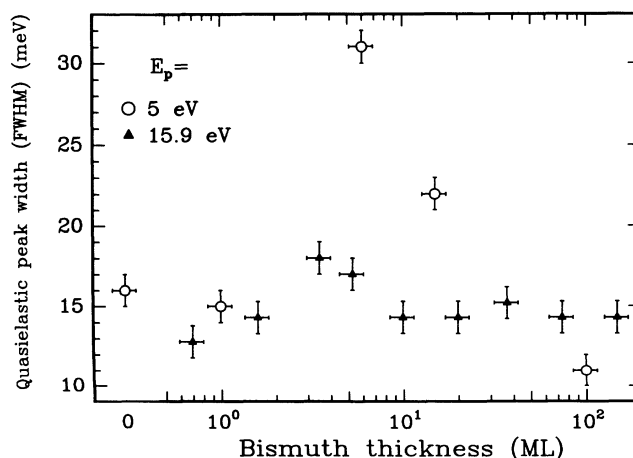


FIG. 5. Quasielastic peak width [evaluated as the full width at half maximum (FWHM)], as a function of the Bi coverage and the primary beam energy ($E_p = 5$ eV, white dots; $E_p = 15.9$ eV, black triangles).

fore be attributed to the diminished order of the surface, partially covered by the epitaxial Bi layer. This is consistent with the LEED observation of a slightly lower sharpness of the spots with respect to the pattern of the clean surface, and with the STM images showing large terraces of one layer height, at submonolayer coverage.¹⁰ When the completion of the first monolayer is ultimated, the surface order becomes greater than for submonolayer coverages, explaining the elastic peak intensity increase between 0.5 and 1 ML. Moreover, the further increase observed can be attributed to the evolution toward a metallic behavior beyond 2 ML, that strongly enhances the surface reflectivity. In fact, as in the ~ 2 –5-ML coverage range the surface order is not increased (the overlayer grows in 3D islands, and the LEED image does not sharpen), but I_0 mounts, we must suppose that the overlayer metallicity increases in this coverage range. Beyond 5 ML both the less ordered surface and perhaps the slightly lower metallicity of the last growth phase reduce the sample reflectivity: in particular, we observed an intensity decrease from 5 to 30 ML, while the Bi crystalline structure evolves from the pseudocubical phase to the bulklike one. Beyond 30 ML the peak intensity reaches a *plateau*, indicating a steady growth of the semimetallic crystal.

We can deepen our analysis of the interface dielectric evolution in a more quantitative way by using a semiclassical dielectric layer model¹⁸ to reproduce the experimental data at different coverages. For this purpose, we have employed a model system built up by several different layers, each described by its peculiar dielectric response. The model GaAs substrate consisted of two layers; a bulk semi-infinite layer and a surface depletion layer. The bulk layer can be described through the dielectric function

$$\epsilon_{\text{GaAs}} = \epsilon_{\infty} + \frac{Q\omega_{\text{ph}}^2}{\omega^2 - \omega_{\text{ph}}^2 - i\gamma_{\text{ph}}\omega} - \frac{\omega_{\text{pl}}^2}{\omega^2 + i\gamma_{\text{pl}}\omega},$$

where ω_{ph} and ω_{pl} are the oscillator frequencies of the Fuchs-Kliwer phonon and the dopant-induced free-carrier plasmon, respectively, while γ_{ph} and γ_{pl} are their phenomenological dampings; ϵ_{∞} is the infrared infinite frequency value of the GaAs dielectric function, and Q is the phonon oscillator strength. The numerical value of these constants, along with all the other parameters in-

troduced during the analysis (which best fit the clean GaAs data) are listed in Table I.²² We remark that an $\omega_{\text{pl}} = 224$ meV corresponds to a surface plasmon $\omega_{\text{pl}}/\sqrt{\epsilon_{\infty} + 1} = 60$ meV, consistent with the experiment, and that the characteristic modes of this layer, deriving from the Coulombian coupling between plasmon and phonon, are called plasmarons (phononlike and plasmonlike branches). The second layer (surface region) reproduces the space-charge region, and differs from bulk GaAs only for the absence of the plasma oscillator. Using this two-layer model and varying only the depletion layer thickness, we were able to reproduce quite well the spectra for the submonolayer coverage region, as shown in Fig. 6, while the use of a third topmost layer representing semiconducting bismuth did not improve the fit. For a Bi thickness lower than 1 ML, the main effect due to the semiconducting overlayer is to increase the depletion layer thickness, influencing both the plasmon and the phonon loss structures. The phonon feature is prevalently determined by the free-carrier depleted region, as the phononlike plasmaron of the underlying bulk is almost completely screened out by the free-carrier gas, while the plasmonlike structure derives from the underlying undepleted region. Therefore, the extension of the depletion layer thickness causes both the enhancement of the phononlike structure intensity and the attenuation of the plasmonlike peak. Moreover, a change in the depletion layer extension determines an energy shift of the plasmon loss structure, since the effective dielectric function of the system $\epsilon_{\text{eff}}(\omega)$ can be written as a combination of the dielectric function of each layer, properly weighted by its thickness.¹⁸ Through the careful fitting of the phonon and plasmon loss structures we could thus evaluate the depletion layer thickness. Within the Schottky barrier approximation we established a band bending value $V_{\text{bb}} = 0.56 \pm 0.02$ eV at the saturation coverage of 1 ML for the higher doped sample, as shown in Fig. 7, in good agreement with other measurements.^{10,14,19} The same evaluation has been made for the $n = 3 \times 10^{16} \text{ cm}^{-3}$ doped sample and gives a value of 0.25 ± 0.1 eV. However, the difficulty in evaluating the plasmon energy shift, which in these spectra is convoluted with the elastic peak, leads to a large percentual error in the estimated value of V_{bb} .

For an overlayer thickness larger than 1 ML, the main features are (i) a strong attenuation of both phonon and

TABLE I. Parameters used for the dielectric model calculation fitting the experimental data. ϵ_{∞} is the infrared infinite frequency value of the GaAs dielectric function; ω_{ph} and ω_{pl} are the phonon and plasmon energies, respectively; γ_{ph} and γ_{pl} are the phonon and plasmon dampings, respectively; and Q is the phonon oscillator strength.

Layer	ϵ_{∞}	ω_{ph} (meV)	γ_{ph} (meV)	Q	ω_{pl} (meV)	γ_{pl} (meV)
GaAs	10.9 ^a	33.4 ^a	0.3 ^a	2.03 ^a	224	10
					$n = 2.7 \times 10^{18} \text{ cm}^{-3}$	22
Depl. layer	10.9 ^a	33.4 ^a	0.3 ^a	2.03 ^a		
semic. Bi	20					
metal. Bi	150				1200	120

^aData taken from Ref. 22.

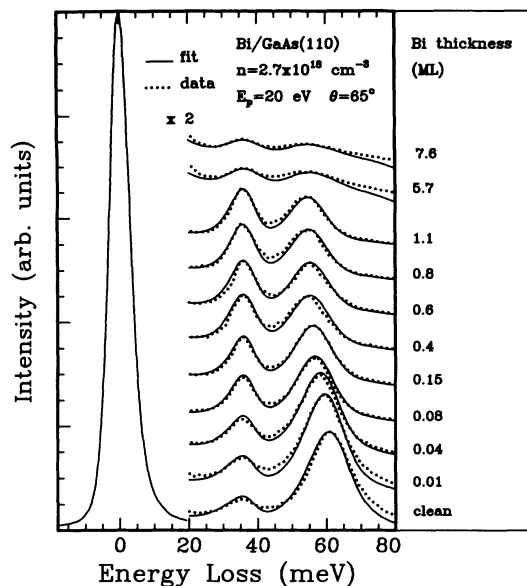


FIG. 6. Experimental HREELS data of the Bi/[*n*-type GaAs(110)] interface system (doping concentration $n = 2.7 \times 10^{18} \text{ cm}^{-3}$), as taken from Fig. 3 (dotted lines). Results of the fitting dielectric model calculation relative to each Bi coverage (continuous lines). Spectra are normalized to their respective quasielastic peak heights, and displaced along the vertical axis for the sake of clarity.

plasmon; (ii) an increase and subsequent decrease of the quasielastic peak width; (iii) a slight backshift of the plasmon energy at a Bi coverage of ~ 5 ML; and (iv) growth of a structureless background beneath the phonon and plasmon structures.

In order to gain further information about the dielectric character of the interface at this coverage state (> 1 ML), we introduced a third (topmost) layer representing bismuth. For coverages between 1 and 2 ML the use of a semiconducting layer (characterized by a constant dielectric function) leads to a good fit of the loss structures, while beyond 2 ML we could not reproduce the spectral

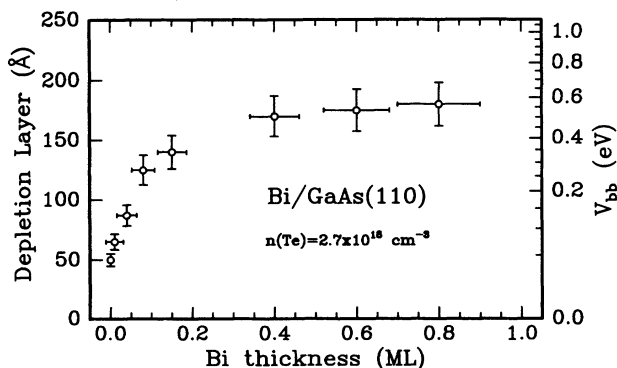


FIG. 7. Band bending potential V_{bb} (right) and depletion-layer thickness (left), as a function of the Bi coverage, for the highly doped substrate ($n = 2.7 \times 10^{18} \text{ cm}^{-3}$). Data deduced from the fitting dielectric model calculations.

changes (peak attenuation rate, backshift of the plasmon, quasielastic peak widening) on considering a simple semiconducting bismuth layer. We had consequently to consider the starting of the metallization above 2 ML.

As we know from previous HREELS,¹³ photoemission,^{9,10} and inverse photoemission^{11,12} measurements, beyond 2 ML the Bi overlayer becomes semimetallic, as the Fermi energy crosses the conduction band and the energy gap closes. However, the very nature of this metallicity is not yet fully understood, as the bismuth layer in this intermediate growth phase results different from semimetallic bulklike Bi. Hence, for fully determining the dielectric nature of the Bi/GaAs(110) system at this coverage stage, we have modeled the interface system by introducing a further (topmost) Bi layer characterized by a metallic Drude-like dielectric function. In this condition, we were able to reproduce fairly well the spectra corresponding to the intermediate coverage stage, varying only the metallic layer thickness, as shown in Figs. 6 and 8, for the lower and higher doped substrates, respectively. The best-fit parameters found for the metallic layer were $\epsilon_{\infty} = 150$ [close to the bulk Bi value of ≈ 100 (Ref. 23)], a plasmon frequency of 1.2 eV, and a damping of 0.12 eV. As a matter of fact, the semiclassical dielectric model gives good fits of the reconstructed spectra to the experimental data, bringing into evidence the interface metallization; however, we would like to point out the intrinsic limitation in the use of such a model in the present physical situation. While the uniform layer model is perfectly suited for the Bi/GaAs(110) interface up to the completion of 1 ML, i.e., in the epitaxial growth phase, it becomes more qualitative when dealing with the higher overlayer thickness. In fact, Bi grows in a Stransky-Krastanov mode, thus the uniform layer approximation

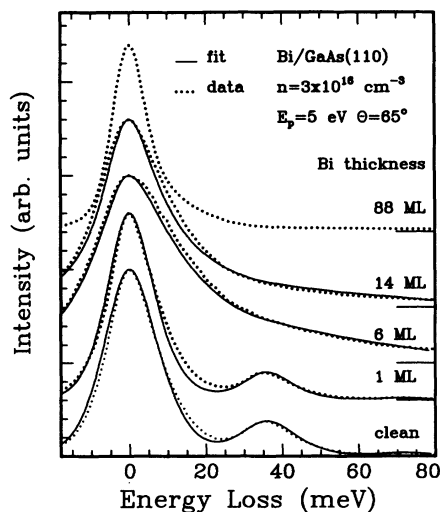


FIG. 8. Experimental HREELS data of the Bi/[*n*-type GaAs(110)] interface system (doping concentration $n = 3 \times 10^{16} \text{ cm}^{-3}$), taken with a primary beam energy of 5 eV and angle of incidence of 65° . Results of the fitting dielectric model calculation relative to each Bi coverage (continuous lines). Spectra are normalized to their respective quasielastic peak heights, and displaced along the vertical axis for the sake of clarity.

is not completely fulfilled above 1 ML. Nevertheless, the model calculation furnishes decisive qualitative indications of the dielectric nature of the system, even at high coverages. That is, the actual physical situation at this coverage stage corresponds—concerning the model calculation—to an *equivalent* uniform layer of semimetallic bismuth with a low density of free electrons. This is also reflected in the quasielastic peak width behavior vs coverage, as the onset of metallicity (marked by the peak enlargement) is at $\approx 6\text{--}9 \text{ \AA}$ Bi, while a full metallization of the overlayer (detectable through the complete screening of the substrate excitations) is achieved for a thickness larger than $\approx 60 \text{ \AA}$. In any event, the conclusion that metallic screening must be taken into account for explaining the experimental data is not affected by the approximation of uniform layers.

Regarding the metallicity of the overlayer in the different growth phases, the behavior of the reflectivity as a function of Bi coverage indicates that in the intermediate growth phase, Bi has a more accentuated metallic character than in the bulklike phase. With reference to this last item, we recall that in this latter phase Bi presents a very low free-carrier density ($3 \times 10^{17} \text{ cm}^{-3}$) for both electrons and holes.²⁴ Moreover, due to a quantum size effect,¹⁶ the bulklike Bi film undergoes a semimetal-semiconductor transition at a thickness of $\sim 100 \text{ \AA}$, so that a thinner Bi film would present an even lower density of free carriers, which cannot account for the dielectric behavior of the intermediate growth phase.

V. CONCLUSIONS

In this paper we have reported and analyzed HREELS measurements for the Bi/[*n*-type GaAs(110)] interface, for a Bi thickness ranging from 0 to 30 ML. In particular, we have studied the dielectric evolution of the system in correspondence to the growth morphology changes, upon increasing the Bi coverage. For submonolayer coverages, the Bi overlayer induces in the GaAs substrate a space-charge region, whose extension has been evaluated fitting the data with the model calculation. From these

values of the depletion layer thickness we have calculated, in the Schottky barrier approximation, the induced band bending potential, that results to be 0.56 eV for a doping level of $n = 2.7 \times 10^{18} \text{ cm}^{-3}$, in good agreement with previous measurements.^{10,14,19} We remark that this determination of the band bending potential, though indirect, has the advantage of being absolutely free from any possible surface photovoltage effects,^{25,26} owing to the extremely low current density reaching the sample (below 1 nA/cm^2). For coverages beyond 2 ML, we observed a metallization of the system, pointed out by both the increase of the elastic-peak intensity and the modifications of the spectral features (width, frequency, and background). An important tool in this investigation has been the use of a semiclassical dielectric layer model, not only to provide information about the space-charge layer, but also to extract the dielectric properties of the system from the HREELS spectra. We were able to reproduce the spectra in this coverage range ($> 2 \text{ ML}$), introducing a Drude-like metallic layer, characterized by a large dielectric constant ϵ_∞ and damping of the plasma oscillator. This kind of dielectric characterization (uniform layers) of the overlayer probably does not fully correspond to the physical situation (island on uniform layers), but nevertheless it can account for the spectral evolution and gives the main result (metallization) without any doubt. We can assert that the Bi overlayer in this thickness range behaves, from the dielectrical point of view, as a uniform layer characterized by a low density of free carriers. Moreover, the behavior of the reflectivity as a function of Bi coverage indicates that, in the intermediate growth phase, Bi has a more accentuated metallic character than in the bulklike phase.

ACKNOWLEDGMENTS

The experimental assistance by Ergisto Angeli is thanked. Financial support to this work came partially from Ministero dell'Università e della Ricerca Scientifica e Tecnologica (MURST) and from Consiglio Nazionale delle Ricerche (CNR).

¹J. Carelli and A. Kahn, Surf. Sci. **116**, 380 (1982).

²M. Mattern-Klosson and H. Lüth, Phys. Rev. B **33**, 2559 (1986).

³W. Pletschen, N. Esser, H. Münder, D. Zahn, J. Geurts, and W. Richter, Surf. Sci. **178**, 140 (1986).

⁴M. Hünermann, W. Pletschen, U. Resch, U. Rettweiler, W. Geurts, and W. Richter, Surf. Sci. **189/190**, 322 (1987).

⁵D. E. Savage and M. G. Lagally, Appl. Phys. Lett. **50**, 1719 (1987).

⁶G. Annovi, Maria Grazia Betti, U. del Pennino, and Carlo Mariani, Phys. Rev. B **41**, 11 978 (1990).

⁷J. C. Patrin, Y. Z. Li, M. Chander, and J. H. Weaver, Phys. Rev. B **46**, 10 221 (1992).

⁸T. Guo, R. E. Atkinson, and W. K. Ford, Phys. Rev. B **41**, 5138 (1990).

⁹J. J. Joyce, J. Anderson, M. M. Nelson, and G. J. Lapeyre,

Phys. Rev. B **40**, 10 412 (1989).

¹⁰R. Ludeke, A. Taleb-Ibrahimi, R. M. Feenstra, and A. B. McLean, J. Vac. Sci. Technol. B **7**, 936 (1989); A. B. McLean, R. M. Feenstra, A. Taleb-Ibrahimi, and R. Ludeke, Phys. Rev. B **39**, 12 925 (1989).

¹¹Y. Hu, T. J. Wagoner, M. B. Jost, and J. H. Weaver, Phys. Rev. B **40**, 11 46 (1989).

¹²A. B. McLean and F. J. Himpsel, Phys. Rev. B **40**, 8425 (1989).

¹³M. G. Betti, M. Pedio, U. del Pennino, and C. Mariani, Phys. Rev. B **45**, 14 057 (1992).

¹⁴N. Esser, M. Hünermann, U. Resch, D. Spaltmann, J. Geurts, D. R. T. Zahn, W. Richter, and R. H. Williams, Appl. Surf. Sci. **41/42**, 169 (1989).

¹⁵V. De Renzi, M. G. Betti, and C. Mariani, Surf. Sci. **287/288**, 550 (1993).

- ¹⁶V. De Renzi, M. G. Betti, and C. Mariani, *Phys. Rev. B* **48**, 4767 (1993).
- ¹⁷H. Ibach and D. L. Mills, *Electron Energy Loss Spectroscopy and Surface Vibrations* (Academic, New York, 1982).
- ¹⁸Ph. Lambin, J.-P. Vigneron, and A. A. Lucas, *Phys. Rev. B* **32**, 8203 (1984).
- ¹⁹J. J. Joyce, J. Anderson, M. M. Nelson, C. Yu, and G. J. Lapeyre, *J. Vac. Sci. Technol. A* **7**, 850 (1989).
- ²⁰R. Fuchs and K. L. Kliewer, *Phys. Rev.* **140**, 2076 (1965).
- ²¹L. H. Dubois, G. P. Schwartz, R. E. Camley, and D. L. Mills, *Phys. Rev. B* **29**, 3208 (1984).
- ²²Z. J. Gray-Grychowski, R. G. Edgell, B. A. Joyce, R. A. Stradling, and K. Woodbridge, *Surf. Sci.* **186**, 482 (1987).
- ²³S. Takano and H. Kawamura, *J. Phys. Soc. Jpn.* **28**, 348 (1970).
- ²⁴J. Rose and R. Shuchardt, *Phys. Status Solidi B* **117**, 213 (1983).
- ²⁵M. Alonso, R. Cimino, and K. Horn, *Phys. Rev. Lett.* **64**, 1947 (1990).
- ²⁶G. D. Waddill, C. M. Aldao, C. Capasso, P. J. Benning, Y. Hu, T. J. Wagener, M. B. Jost, and J. H. Weaver, *Phys. Rev. B* **41**, 5960 (1990).